https://doi.org/10.5194/egusphere-2026-4846
Preprint. Discussion started: 10 September 2026
© Author(s) 2026. CC BY 4.0 License.

Seasonal Evolution of Alpine Snow Stratigraphy: Multi-Year High-Resolution SnowMicroPen Measurements at Weissfluhjoch

Leah Gaillard-Festa [1], Bettina Richter [1], Lars Mewes [1], Matthias Jaggi [1], and Benjamin Walter [1]

[1]WSL Institute for Snow and Avalanche Research SLF, CH-7260 Davos Dorf, Switzerland

Correspondence: Benjamin Walter (benjamin.walter@slf.ch)

Abstract. Snow density and specific surface area are key properties controlling snowpack mechanical behavior, thermal conductivity, and snow metamorphism. They are crucial parameters in several fields, including avalanche prediction, snow hydrology, and climate modeling. Yet long-term high-resolution in situ observations of their seasonal evolution remain rare. Here we present a ten-year record of daily SnowMicroPen (SMP) measurements collected at the WSL Institute for Snow and Avalanche Research (WSL/SLF) Weissfluhjoch research site (2536 m a.s.l., Davos, Switzerland) spanning winters 2015-2016 to 2024-2025. The SMP measures resistance penetration force and, through parametrization, allows retrieval of density and specific surface area (SSA) at high vertical (millimeter) resolution. Comparison against independent measurements (density cutter, IceCube, etc.) reveals two systematic sources of error. First, an offset in the SMP force signal causes an overestimation of new snow density, and second, temperatures above -0.6 ± 0.2°C result in a strong nonphysical increase in SSA. The overall SMP measurement uncertainties are $40.1\,\mathrm{kg\,m^{-3}}$ for density and $7.05\,\mathrm{m^2\,kg^{-1}}$ for SSA, both in close agreement with previous studies, supporting existing parameterizations to remain valid. The presented 10-year SMP measurements reveal seasonal and inter-annual densification and SSA evolution of alpine snow stratigraphies at unprecedented temporal and spatial (vertical) resolution, providing a unique dataset for improved theoretical descriptions of snow metamorphism, snow optical and mechanical properties, and snowpack model development.

1 Introduction

Understanding snow properties such as density, stratigraphy, and microstructure is necessary in several fields, including avalanche prediction (Schweizer et al., 2003; Van Herwijnen and Jamieson, 2007), snow hydrology (Dozier et al., 2016), and applications in climate simulations (Poschlod and Daloz, 2024). Among these, snow density and specific surface area (SSA) are important physical properties that influence the mechanical characteristics and thermal conductivity of the snowpack and snow layers (Bormann et al., 2013). These properties evolve over time as a result of processes such as isothermal, temperature gradient, and wet snow metamorphism (Legagneux et al., 2004; Calonne et al., 2014), or mechanical compaction due to wind (Walter et al., 2024; Liston et al., 2007) or to snow load (Miot et al., 2025). Because snowpack density and SSA vary in time and space, both vertically and horizontally, measuring snow density and SSA at high temporal and vertical resolution is necessary but remains challenging. Most existing measurements come from short field campaigns or laboratory experiments, limiting the ability to investigate the seasonal evolution of snow properties and their variability between winters. Long-

https://doi.org/10.5194/egusphere-2026-4846
Preprint. Discussion started: 10 September 2026
© Author(s) 2026. CC BY 4.0 License.

term time series are therefore important for improving the understanding of snow metamorphism in natural environments, validating snowpack models, and linking the differences between laboratory-based measurements and real snowpack processes. However, long-term observations of snow properties under natural conditions remain rare. Many instruments are used to measure snow density, including density cutters (Carroll, 1977; Conger and McClung, 2009; Proksch et al., 2016), snow core samplers (Kaasik et al., 2023), and optical-based systems such as the SnowImager (Mewes et al., 2026; Matzl and Schneebeli, 2006). These methods usually depend on measurements of snow mass and volume or optical characterization of the snow structure. SSA can be measured using approaches that rely on the interaction of light with the snow microstructure, such as IceCube (Zuanon, 2013; Gallet et al., 2009), InfraSnow (Gergely et al., 2014), or the SnowImager (Mewes et al., 2026). Reference measurements of SSA are commonly obtained using adsorption of gas (Legagneux et al., 2002; Dominé et al., 2001), while micro-computed tomography allows direct determination of both snow density and SSA from the reconstructed three-dimensional microstructure (Hagenmuller et al., 2016; Heggli et al., 2011; Proksch et al., 2016) and is often considered the most accurate reference. These methods usually give valuable information on snow properties; however, they are generally time-consuming to acquire, have limited vertical resolution, and provide only sparse temporal sampling.

The Weissfluhjoch (WFJ) experimental site in the Swiss Alps provides a unique environment for long-term snow research. The site hosts operational snow and meteorological observations maintained by the WSL Institute for Snow and Avalanche Research SLF in collaboration with MeteoSwiss. Continuous snow measurements have been conducted there since 1936, making it one of the longest-running snow observation sites worldwide. The SnowMicroPen (SMP), developed by the WSL Institute for Snow and Avalanche Research SLF (WSL/SLF) (for Snow and Avalanche Research SLF, 2023), solves this high-resolution challenge in the vertical direction of the snowpack by measuring the penetration resistance force at a vertical resolution of 1/242 mm. Unlike traditional manual sampling, the SMP measures fine vertical variations in snow properties and allows rapid and repeated measurements over time.

The SMP force signal can be interpreted in terms of underlying snow microstructure using the shot noise model approach developed by Johnson and Schneebeli (1999) and Löwe and van Herwijnen (2012). Characteristic micromechanical parameters are obtained, including a median force (F_m) and a characteristic length (L), which describes the configuration of these structural elements. These micro-parameters are then used to obtain snow density and SSA using parametrization such as the one developed by Proksch et al. (2015) or the one refined by Calonne et al. (2020). At the Weissfluhjoch research site, PhD students from the WSL Institute for Snow and Avalanche Research (SLF) have conducted daily snow measurements using the SMP since 2015. This has produced a valuable multi-year dataset spanning over ten winters, providing detailed insight into the time evolution of snowpack properties and the core physical processes driving snow structure and metamorphism. In this paper, we present a 10-year dataset of daily SMP measurements collected at the Weissfluhjoch site. We first describe the SMP measurements, reference datasets, and processing methodology. We then compare SMP-derived density and SSA with independent reference measurements and investigate the influence of signal offset and snow temperature on the retrievals. Finally, we discuss the implications of these effects for long-term SMP observations and for characterizing seasonal and inter-annual snowpack evolution.

https://doi.org/10.5194/egusphere-2026-4846
Preprint. Discussion started: 10 September 2026
© Author(s) 2026. CC BY 4.0 License.

2 Methods

2.1 Field site

The Weissfluhjoch test site is located on a flat field, in the Swiss Alps above Davos, Switzerland, at an elevation of 2536 m a.s.l. (46.82963° N, 9.80925° E) (Fig. 1). The WSL/SLF operates it in collaboration with MeteoSwiss, and it provides long-term datasets of snow and meteorological conditions. Manual measurements are performed daily and include observations such as snow depth, new snow height, snow water equivalent (SWE), and SMP measurements for density and SSA retrieval. In addition, an automated meteorological station (IMIS (Intercantonal Measurement and Information System IMIS, 2023)) records meteorological values continuously, including air temperature, wind speed, humidity, and incoming radiation. Additional instrumentation at the site includes devices such as snow pillows and snow scales, which provide continuous measurement of snow mass. Twice a month, a detailed snow profile is performed. This consists of snow layer classification, penetration resistance data, snow temperatures, and the snow water equivalent of the full snowpack.

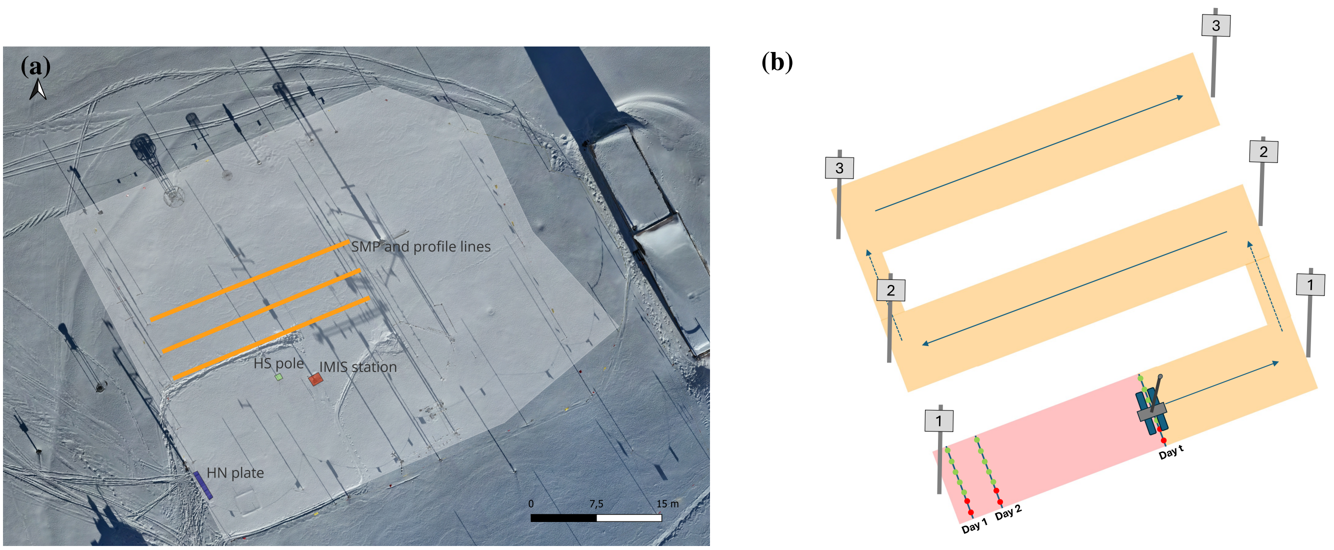

Figure 1. (a) Weissfluhjoch test site with the instrument layout plan. Map made with QGIS and orthophoto from 06.01.2026 taken by Andreas Stoffel. **(b)** Schematic representation of the SMP and snow profile field layout. The orange area indicates the undisturbed measurement zone, while the red area represents previously sampled regions. Each day, the SMP performs two cool-down measurements (red dots) followed by five measurement profiles (green dots)

2.2 SnowMicroPen

The SnowMicroPen (SMP) is a high-resolution probe equipped with a force sensor at its tip. It penetrates the snowpack at a constant speed (20mm/s) to measure vertical penetration resistance at a vertical resolution of 4 µm (for Snow and Avalanche Research SLF, 2023). Over the 10 years, versions 4 and 5 of the SMP have been used. At the WFJ, PhD students from

https://doi.org/10.5194/egusphere-2026-4846
Preprint. Discussion started: 10 September 2026
© Author(s) 2026. CC BY 4.0 License.

WSL/SLF conduct SMP measurements daily between 07:30 and 08:00 am, until the snow cover becomes too shallow or too hard for profiling. Measurements began in November 2015, and the time series is still ongoing. Here we analyze the first 10 years from November 2015 to April 2025. Each winter, profiles are acquired at a fixed location within the site (Fig. 1a). Measurements are performed along predefined sampling lines to ensure that each profile is acquired in undisturbed snow. The first two daily profiles are used to cool down the instrument, while the following measurements are then considered valid. Raw data from an individual SMP profile are stored in binary PNT files. An expert performed manual quality control on all SMP files, including detection of the snow surface. Metadata, such as snow surface markers, are stored in accompanying .INI files. From these SMP force measurements, SSA and density were obtained based on the statistical framework and approach described in Section 2.5. The SMP dataset analyzed in this study is publicly available via EnviDat (Löwe et al., 2025).

2.3 Manual observations

Manual observations of snow depth (HS) and new snow depth (HN) are conducted every day at 8 am (UTC+1). Snow depth is measured using a fixed graduated pole (HS pole in Fig. 1a), while new snow depth is determined every morning from the fresh 24-hour snowfall accumulation on a snow board placed at the site and cleared after each measurement (Fierz et al., 2009) (HN plate in Fig. 1a). Every two weeks, a full manual snow pit is dug following the SMP measurements. This detailed snow profiling records temperature, snow water equivalent (SWE), hardness, grain size, and type. These measurements are performed at the same location as the SMP profiles, along the same profile lines (Fig. 1a).

Density Cutter

Density cutters are a gravimetric measurement in which density is derived by weighing a known volume of snow which is extracted from the profile using a rectangular cutter of 100 cm^3 (Carroll, 1977; Conger and McClung, 2009; Proksch et al., 2016). Measurements start at the snow surface and extend to the bottom, and have a vertical resolution of 3 cm. These measurements were conducted approximately every two weeks for the winter 2015-2016 and 2016-2017 as part of the RHOSSA campaign conducted by Calonne et al. (2020) to derive the empirical SMP parameterization for snow density.

New snow density

Fresh snow is measured using a white board aligned with the snow surface; each morning, the new snow depth (HN) accumulated during the previous 24 hours is measured with a ruler on the board (Fierz et al., 2009). A cylindrical metal sampler of area A=1000 cm^2 is placed on the snow collected on the board and weighed on a high-precision electronic scale to retrieve the 24-hour snow mass (m_{snow}). Manually observed new snow densities (ρ_{HNW}) are then computed from HN and SWE (SWE_{HN}= $\frac{m_{snow}}{A \cdot \rho_{\mathrm{water}}}$ mm) of the new snow:

$$\rho_{\mathrm{HNW}} \ \ [\mathrm{kg\,m^{-3}}] = \frac{SWE_{\mathrm{HN}} \ \ [\mathrm{mm}] \cdot 1000 \ \ [\mathrm{kg\,m^{-3}}]}{HN \ \ [\mathrm{mm}]} \tag{1}$$

New snow events with little snow height (HN<2cm) result in inaccurate new snow density values and were therefore excluded from the dataset. The data of HN and corresponding SWE values are available on EnviDat (Magnusson and Jonas, 2025).

https://doi.org/10.5194/egusphere-2026-4846
Preprint. Discussion started: 10 September 2026
© Author(s) 2026. CC BY 4.0 License.

IceCube

IceCube provides an optical method for retrieving SSA based on the reflectance of near-infrared light (Zuanon, 2013; Gallet et al., 2009). IceCube measurements were performed similarly to the density cutter, starting at the surface and extending to the bottom of the snowpack with a height resolution of 3 cm. Profiles were collected every two weeks during the winters of 2015–2016 and 2016–2017 as part of the RHOSSA campaign (Calonne et al., 2020), where these measurements were used to derive a parameterization relating SMP force signals to SSA at the WFJ site.

Bi-monthly SWE profiles

These data are part of the Global Climate Observing System (GCOS, (Marty, 2020)), where SWE measurements of the entire snowpack are obtained using SWE snow-core samplers, which are inserted vertically from the surface into the snowpack and are recorded bi-monthly (Marty et al., 2023). These measurements, along with the recorded snow height, can be used to derive the vertically averaged snow density ρ_{HS} (Similar to Eq. 1). This dataset provides information on the SWE of the entire snowpack over the winter season. The data used in this paper span 2015 to 2025.

Bi-monthly temperatures

The manual temperature profiles were typically recorded at a vertical resolution of 10 cm from the surface to the ground. The thermometers used to measure snow temperature have an accuracy of ± 0.2°C. Manual snow temperature profiles were retrieved from the WSL/SLF's CAAML (Canadian Avalanche Association Markup Language) archive. These files provide metadata for standardized snow observations according to IACS standards (International Association of Cryospheric Sciences) (Fierz et al., 2009). To relate these measurements to other instrument data (SMP and IceCube/Cutter), we applied a two-step resampling procedure. We started by interpolating the 10 cm discrete temperature measurements to obtain a continuous temperature profile. To ensure vertical consistency, we aligned the upper boundary of each profile with the measured HS at the time of observation, then resampled to either 0.5 mm to match the SMP or 3 cm to match the cutter and IceCube.

2.4 Automated weather station

The automated measurement station (Intercantonal Measurement and Information System IMIS, 2023) measures air temperature, humidity, wind, reflected radiation, precipitation, and specific snowpack parameters, such as total snow height, the temperature of the snow surface measured from thermal radiation, and the snow temperature at heights 0, 25, 50, and 100 cm from the ground measured by a temperature sensor. These data are collected daily at a temporal resolution of 30 minutes. The location of the IMIS station is shown in Fig. 1. The data are publicly available on EnviDat at (Fierz, 2019).

2.5 SMP processing

To prepare the daily SMP profiles, an expert first labeled each of the five SMP measurements with quality flags 1 and 2, based on a visual inspection of the entire profile and an assessment of signal drift and offset during the initial air measurement before the

https://doi.org/10.5194/egusphere-2026-4846
Preprint. Discussion started: 10 September 2026
© Author(s) 2026. CC BY 4.0 License.

Table 1. Overview of instrumentation and sampling protocols for the 10-year WFJ dataset (2015–2025).

Instrument	Measured/Derived Quantity	Vert. Res.	Frequency	Period
SMP	Force (N); ρ_{SMP} ($\mathrm{kg\,m^{-3}}$); $\mathrm{SSA_{SMP}}$ ($\mathrm{m^2\,kg^{-1}}$)	0.5 mm	Daily	2015–2025
Density cutter	ρ_{cutter} ($\mathrm{kg\,m^{-3}}$)	3 cm	Bi-monthly	2015–2017
SWE column	SWE (mm), ρ_{HS} ($\mathrm{kg\,m^{-3}}$)	HS height	Bi-monthly	2015–2025
HN board	HN (mm), ρ_{HNW} ($\mathrm{kg\,m^{-3}}$)	HN height	Event-based	2015–2025
IceCube	$\mathrm{SSA_{IC}}$ ($\mathrm{m^2\,kg^{-1}}$)	3 cm	Bi-monthly	2015–2017
Temperature probe	Snow temperature (TS, °C)	≈10 cm	Bi-monthly	2015–2025
IMIS temperature and thermal radiation sensors	$TSS, TS_{25}, TS_{50}, TS_{100}$ (°C)	Fixed heights	10 min	2015-2025

force sensor penetrated the snow. Previous SMP processing generally assumed the signal offset to be negligible and therefore did not apply an offset correction. In this study, we quantified and corrected the offset, and we evaluate the implications of this correction in Section 3.2. For each profile, the drift and offset were computed using a linear fit to the force signal over a stable period of the signal measured in the air. When available, the markers drift_begin and drift_end were directly used to define the drift interval. If these markers were absent, the drift region began after excluding the first 10 data points and ended at the surface marker or the last sample if no marker was present. A linear regression was then applied to the force values within this interval, and the resulting offset was subtracted from the full force profile such that the air portion of the corrected signal matched the mean RHOSSA offset of 15.3 mN. An example of drift and offset is shown in Fig. 2a from 16 April 2024 (File: S36N2659.PNT), where the initial portion of the signal corresponding to measurements taken in air is highlighted in the zoom-in window to illustrate how offset and drift are identified in the force signal. The computed offsets for winter 2015-2025 are shown in Fig. 2b.

From the SMP force profiles, SSA ($\mathrm{m^2\,kg^{-1}}$) and density ($\mathrm{kg\,m^{-3}}$) are computed according to the parametrization derived by Calonne et al. (2020) (CR2020).

$$\rho_{\mathrm{SMP}} = 295.8 + 65.1\ln(F_{\mathrm{m}}) - 43.2\ln(F_{\mathrm{m}})L + 47.1L \quad (2)$$

$$SSA_{\mathrm{SMP}} = 0.57 - 18.56\ln(L) - 3.66\ln(F_{\mathrm{m}}) \quad (3)$$

Here, F_{m} and L are derived using a sliding window of 1 mm with 50 % overlap, as suggested in Calonne et al. (2020), resulting in a smoothed force profile with a vertical resolution of 0.5 mm. Within each window, median force F_{m} ($\mathrm{kg\,m^{-3}}$) and structural element size L (mm) are computed using the shot noise model described in Löwe and van Herwijnen (2012), where L can be interpreted as the spatial correlation of rupture events and therefore be understood as the mean distance between neighboring elements or snow grains. Please note that the parameterizations for SSA and density (CR2020) were derived from the data of one winter season (2015-2016).

https://doi.org/10.5194/egusphere-2026-4846
Preprint. Discussion started: 10 September 2026
© Author(s) 2026. CC BY 4.0 License.

We computed F_{m} and L profiles from the five daily SMP measurements. To this end, we aligned SMP profiles at the snow surface, using manually measured snow heights (HS) as a common reference. With this, we obtained better results than using the ground as a benchmark, for several reasons. These include the SMP overload protection mechanism (42 N), which can also stop measurements when hard layers e.g., ice lenses are present, ground surface irregularities, and, during winters with substantial snowfall, insufficient length to probe the full snow depth (probe length = 2.1 m or 2.6 m depending on winters). Each aligned SMP profile was processed individually following the procedure described above. For each measurement day, the resulting profiles of F_{m}, L, ρ_{SMP}, and SSA_{SMP} were then aggregated by taking the median at each vertical position, resulting in a single representative daily profile of each parameter. Unless stated otherwise, all analyses presented in this study are based on these representative daily profiles.

SMP measurements were compared with reference measurements, such as density cutter, SWE-derived densities, IceCube-derived SSA values, and snow temperature. To enable consistent comparison, we matched the temporal and vertical resolution of all datasets. For each measurement technique, the upper boundary of the profile was aligned to match HS. The SMP profiles were then resampled to match the vertical resolution of the corresponding instruments. To compare manually observed new snow density (ρ_{HNW}) with SMP density of the new snow (ρ_{SMP}), the new snow layers in the SMP profile were automatically determined using manually observed HN values. To avoid edge effects from denser snow layers, we reduced the new-snow height to 80% of HN and computed the median density.

Agreement between SMP-derived and reference measurements is evaluated using Pearson correlation coefficient (r), concordance correlation coefficient (CCC), and root mean square error (RMSE). While the Pearson correlation coefficient (r) indicates the strength of the linear relationship, it does not account for deviations from the 1:1 agreement line. The concordance correlation coefficient (CCC) combines measures of precision and accuracy by assessing both the correlation and the deviation from the 1:1 line. RMSE provides the average distance between the model's predicted values and the reference values.

https://doi.org/10.5194/egusphere-2026-4846
Preprint. Discussion started: 10 September 2026
© Author(s) 2026. CC BY 4.0 License.

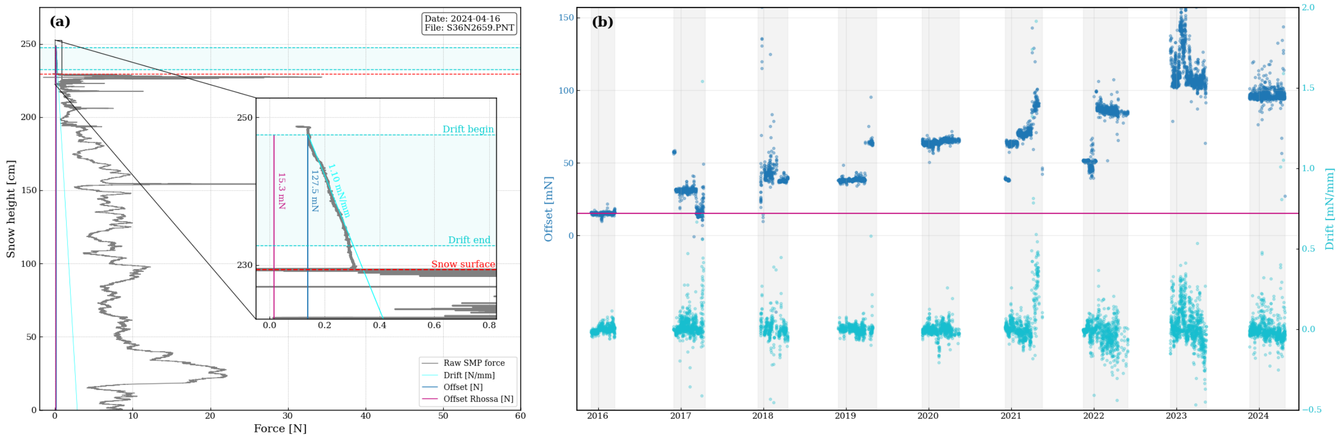

Figure 2. (a) Raw SMP force profile from 16 April 2024, with an inset showing the corresponding drift and offset values, as well as the RHOSSA-derived offset used as the reference for the correction. The highlighted turquoise band marks the depth interval where drift and offset were calculated. **(b)** Time series of the offset and drift from winter 2015-2015. Shaded areas indicate the winter periods. A constant offset derived from (Calonne et al., 2020) is shown for reference (pink line).

3 Results

3.1 Comparison to reference measurements

Fig. 3 compares SMP-derived snow density (Fig. 3a) and SSA (Fig. 3b) against independent reference measurements over different winters. Agreement is strong for both variables and both winters. When comparing SMP density to cutter measurements, the winter season 2015-2016 (r $= 0.90$, CCC $= 0.89$, RMSE $= 39.4\,\mathrm{kg\,m^{-3}}$) performed better then the winter season 2016-2017 (r $= 0.84$, CCC $= 0.70$, RMSE $= 61.2\,\mathrm{kg\,m^{-3}}$), as the parameterization was derived with the data from 2015-2016. Above $250\,\mathrm{kg\,m^{-3}}$ SMP densities show a systematic underestimation relative to the cutter data (see Sec. 4.4). Excluding those data points, the performance increased to r $= 0.84$, CCC $= 0.80$, RMSE $= 42.5\,\mathrm{kg\,m^{-3}}$ and hence almost reaches the RHOSSA stated values. Note that after correcting the surface markers for winter 2015-2016, the RMSE in this study differs slightly from the RMSE reported in Calonne et al. (2020). For SSA, the training winter 2015-2016 (r $= 0.89$, CCC $= 0.84$, RMSE $= 7.8\,\mathrm{m^2\,kg^{-1}}$), performed slightly better than 2016-2017 (r $= 0.83$, CCC $= 0.79$, RMSE $= 8.4\,\mathrm{m^2\,kg^{-1}}$).
In the raw SMP retrievals, densities are systematically overestimated relative to HNW-derived new snow density measurements (light grey data in Fig. 3a, resulting in a large deviation from the 1:1 relationship (RMSE $= 66.1\,\mathrm{kg\,m^{-3}}$, CCC $= 0.26$). Applying the offset correction substantially improves the agreement (Fig. 3a), reducing the RMSE to $40.8\,\mathrm{kg\,m^{-3}}$ and increasing the CCC to 0.53. Nevertheless, the HNW comparison remains the weakest among all reference datasets, with continual deviations from the 1:1 relationship motivating the offset analysis presented in Section 3.2. Similarly, SMP-derived SSA continues to underestimate high values ($> 40\,\mathrm{m^2\,kg^{-1}}$) associated with freshly deposited, low-density and high SSA snow.
At high densities ($> 300\,\mathrm{kg\,m^{-3}}$), the SMP tends to underestimate density relative to cutter measurements. The affected

https://doi.org/10.5194/egusphere-2026-4846
Preprint. Discussion started: 10 September 2026
© Author(s) 2026. CC BY 4.0 License.

samples are concentrated in measurements acquired after 10 March 2017 and are also largely associated with snow temperatures above $-0.6°C$ (highlighted in pink in Fig. 3). Excluding these warm samples leaves agreement metrics largely unchanged for 2015-2016 but clearly improves them for 2016-2017. For SSA, the increased scatter at low values ($< 20\,\mathrm{m^2\,kg^{-1}}$) in 2016-2017 is mainly associated with warmer conditions; removing these samples reduces RMSE from 8.4 to $5.79\,\mathrm{m^2\,kg^{-1}}$ with concurrent improvements in r and CCC. Section 3.3 investigates the temperature-dependent nature of the deviations. Considering all available reference datasets (density cutter, HN board, SWE column, IceCube), the overall density RMSE is $47.2\,\mathrm{kg\,m^{-3}}$. Excluding the anomalous March 2017 subset reduces the RMSE to $40.1\,\mathrm{kg\,m^{-3}}$, which is close to the value of $34\,\mathrm{kg\,m^{-3}}$ reported in the RHOSSA study despite including HNW density dataset. For SSA, combining both winters after excluding snow with temperatures above -0.6°C resulted in an overall RMSE of $7.05\,\mathrm{m^2\,kg^{-1}}$, essentially identical to the $7\,\mathrm{m^2\,kg^{-1}}$ reported in the RHOSSA study.

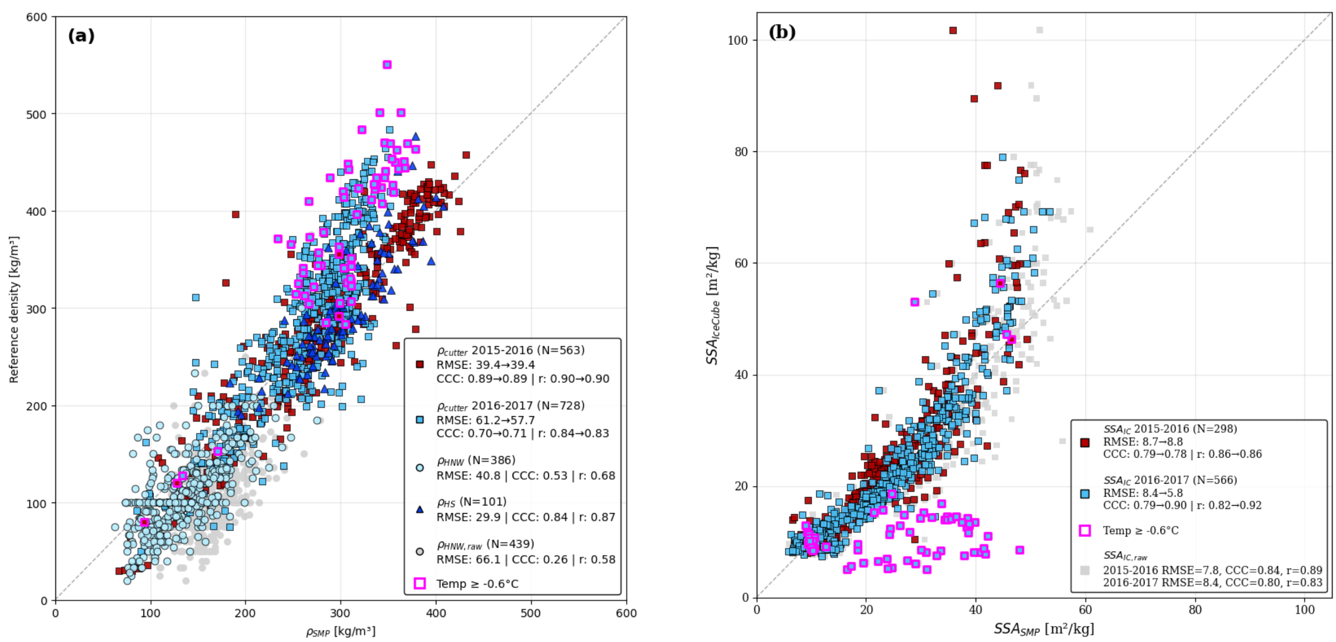

Figure 3. (a) Comparison of SMP-derived density with reference measurements, including density cutter observations, density derived from SWE measurements, and new snow density from HN board measurements. **(b)** Comparison of SMP-derived SSA with IceCube measurements from winters 2015-2016 and 2016-2017. Metrics before and after the arrow correspond to the full dataset and to the dataset excluding the highlighted observations with snow temperatures above $-0.6°C$, respectively. Light grey symbols represent the raw SMP derived density and SSA prior to offset correction, while colored symbols show the offset-corrected retrievals referenced to the RHOSSA mean offset.

3.2 Offset and drift

The fresh snow deviations identified in Section 3.1 motivated an investigation of the SMP baseline offset. Fig. 2a shows the raw force signal on 16 April 2024, including offset and drift of the air signal. The offset of $127.5\,\mathrm{mN}$ is almost 10 times larger

https://doi.org/10.5194/egusphere-2026-4846
Preprint. Discussion started: 10 September 2026
© Author(s) 2026. CC BY 4.0 License.

than the average offset of the RHOSSA ($15.3\,\mathrm{mN}$). Fig. 2b illustrates the time evolution of these quantities over the ten years. The gray shaded areas indicate the start and end of individual winter seasons, and the pink line represents the mean offset value for the 2015–2016 winter season. Force measurements in air revealed a clear winter-dependent offset, which increased systematically over the ten years. Because this offset showed consistent behavior spanning years, applying a correction was important to ensure comparability of SMP profiles between winters. In contrast, the drift component did not exhibit a systematic trend with year and varied randomly between winters. Although a drift correction was evaluated, it had a negligible effect on the processed force signal and was therefore not applied in the final processing. We chose to correct the offset to the RHOSSA offset of $15.3\,\mathrm{mN}$ as the parameterizations for SSA and density (Eq. 2 and 3) were not designed to work with near-zero force values. Correcting the force signal to zero occasionally yielded negative or near- zero force values for snow layers with low force resistance. As a result, the logarithmic transformations in the parameterizations are not possible or produce unrealistic values.

To illustrate the impact of the offset correction on SMP-derived density and SSA, winter 2023–2024 was selected as a representative example (Fig. 4), as it exhibited one of the largest mean offsets of the study period ($96.6\,\mathrm{mN}$). Differences were computed between the uncorrected data and data corrected relative to the mean offset of the 2015–2016 reference winter. The impact of the offset correction on the entire snowpack can be observed for the median force (F_m) in Fig.4a, for L in Fig. 4b, for density in Fig. 4c, and for SSA in Fig. 4d. The offset introduces a systematic bias in the SMP force signal, resulting in a nearly uniform shift in F_m within individual daily profiles. As a consequence, the correction results in a vertically homogeneous adjustment of F_m, which is especially marked in winters with large offsets, such as 2023–2024. In contrast, L exhibits layer-dependent changes to the offset correction. Changes in L are heterogeneous across the snowpack, with the largest variations occurring in lower force layers. The offset correction has its largest impact on derived parameters in the upper snowpack. These layers show comparatively low force values and therefore experience large relative changes in both F_m and L after correction. Those variations transfer to the obtained density and SSA. As a result, uncorrected data systematically overestimate both density and SSA. This effect is most pronounced in low-density, high-SSA fresh snow. Differences in SSA reach up to approximately $10\,\mathrm{m}^2\,\mathrm{kg}^{-1}$ and in density up to $50\,\mathrm{kg}\,\mathrm{m}^{-3}$ with corresponding reductions after correction. However, the systematic underestimation of high SSA values (Fig. 3) persists after correction.

https://doi.org/10.5194/egusphere-2026-4846
Preprint. Discussion started: 10 September 2026
© Author(s) 2026. CC BY 4.0 License.

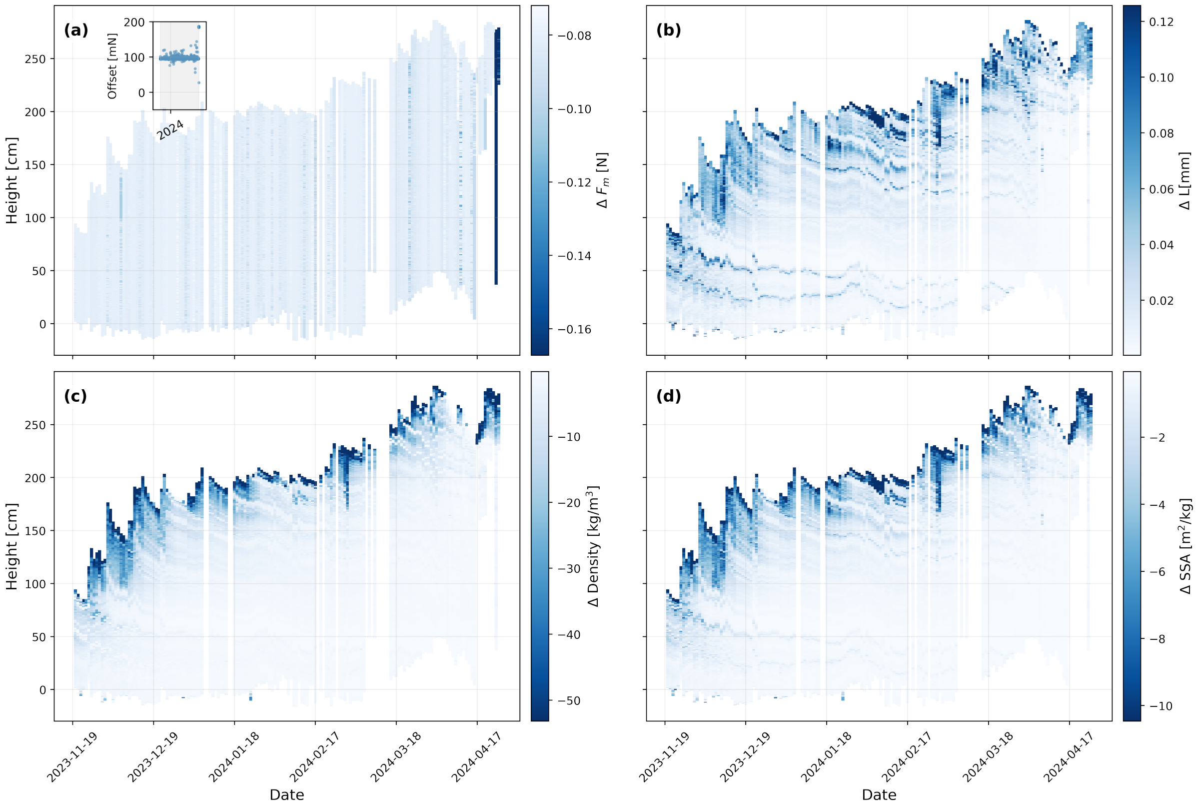

Figure 4. (a) Differences in SMP median force, (b) length scale, (c) density, and (d) SSA between offset-corrected to RHOSSA and uncorrected measurements for the winter 2023–2024. Each panel shows the time evolution of differences (color) with snow height. The inset in panel a) displays the corresponding offsets for that winter.

3.3 Temperature effect on micromechanical parameters

The second systematic deviation identified in Section 3.1 concerns warm snow conditions. As snow temperatures approach 0°C, SMP-derived density underestimates reference cutter values at high densities, while SSA is overestimated relative to IceCube measurements (Fig. 3). Removing samples above -0.6°C substantially improves the agreement of metrics, especially for 2016-2017, pointing to the fact that SMP density and SSA are not accurate near-zero conditions. Fig. 5 shows the behavior of parameters by looking at their median values of L (Fig. 5a), F_{m} (Fig. 5b), and derived SSA and density (Fig. 5c) with manually measured temperature. For temperatures below approximately -6 °C, the L shows little variation with temperature. Above this threshold, L increases with temperature, likely because of enhanced snow metamorphism resulting in different grain types and snow coarsening. However, at -0.6 °C, a sudden decrease in L is observed. A similar behavior is found for F_{m}. At low temperatures (< -6 °C), force values remain relatively low. As temperature increases, F_{m} generally increases, but near -0.6 °C, it rises sharply before decreasing again. The observed changes in L and F_{m} propagate differently into the obtained SMP density and SSA. In the CR2020 parameterization (Eq. 2 and 3), the decrease in L tends to increase SSA wherever the

https://doi.org/10.5194/egusphere-2026-4846
Preprint. Discussion started: 10 September 2026
© Author(s) 2026. CC BY 4.0 License.

increase in F_m acts in the opposite direction. Because the influence of L is substantially larger, the net effect is a pronounced increase in retrieved SSA near-0.6 ± 0.2°C. In contrast, the density retrieval exhibits only a small deviation. In contrast, SSA shows a marked increase associated with the abrupt decrease in L at the same temperature range. Thus, samples warmer than approximately -0.6 ± 0.2°C show greater disagreement between SMP-derived SSA and the reference measurements (Fig. 3). These results identify the -0.6 ± 0.2°C range as the upper temperature limit at which the current SMP processing allows for consistent estimates in the analyzed dataset.

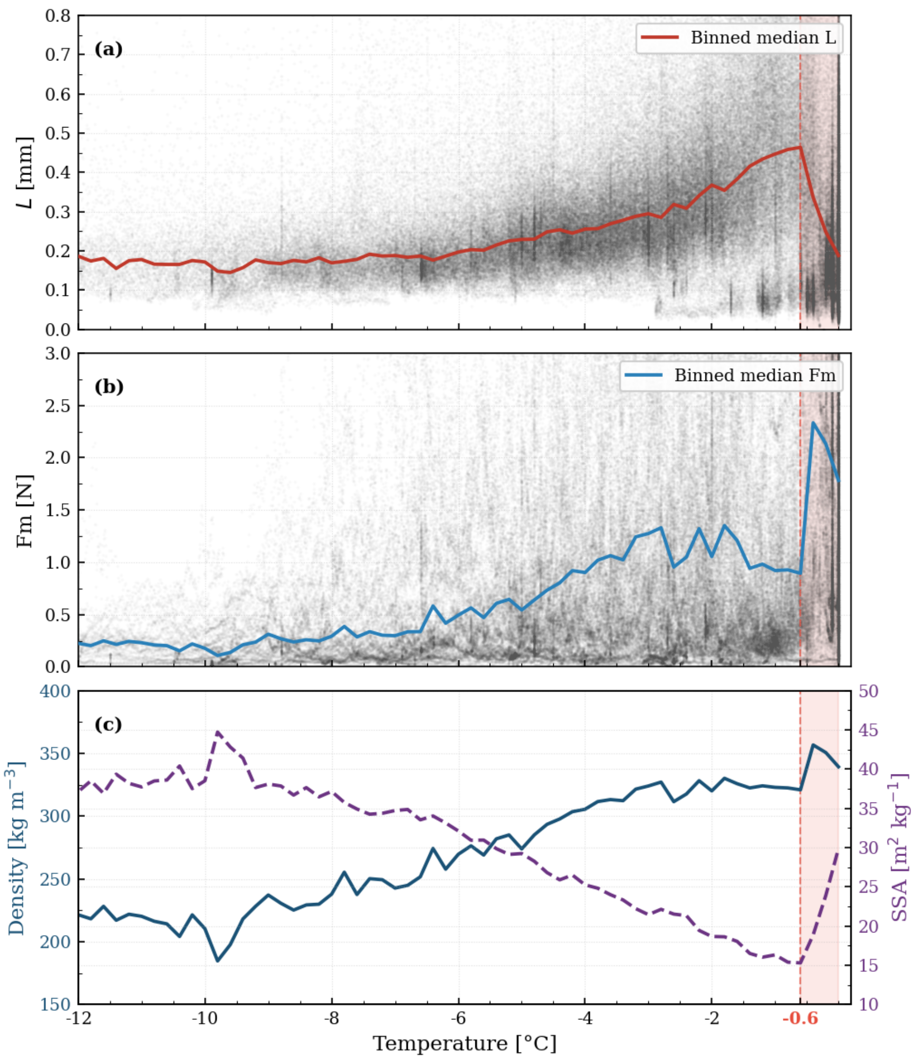

Figure 5. Median values of (a) the microstructural length scale (L), (b) the median penetration force (F_m), and (c) SMP-derived density and specific surface area (SSA) are shown as a function of snow temperature. Grey points represent the individual measurements, while the solid lines show the median values computed within 0.2°C temperature bins. The shaded interval indicates the temperature range around -0.6 ± 0.2°C, where L reaches a maximum and F_m exhibits abrupt changes.

https://doi.org/10.5194/egusphere-2026-4846
Preprint. Discussion started: 10 September 2026
© Author(s) 2026. CC BY 4.0 License.

3.4 10 years overview

For visualization, plotting daily SMP profiles in chronological order does not allow a natural understanding of snowpack evolution, including new snow accumulation, settling, and layer changes. While alignment using HS gives consistency for quantitative analysis, additional adjustments were needed to improve interpretation when visualizing the time series. Therefore, manual alignment was applied for visualization, using only the profile labeled as the best of the day, and it was shifted slightly (mostly between +/- 10 cm) upward or downward to enhance the continuity of force signals between consecutive days. This procedure facilitates clearer visualization of snowpack evolution. Having established the correction procedures and their limitations, Fig. 6 presents the complete offset-corrected SMP dataset, showing the seasonal evolution of SMP-derived snow density and SSA over the ten winters from 2015-2016 to 2024-2025 together with snow height and temperatures measured at different depths within the snowpack. Temperature profiles, together with snow surface temperature from the IMIS station, illustrate the seasonal evolution of temperature changes in the snowpack. Top-layer temperatures show high variability because of atmospheric forcing, while subsurface temperatures become increasingly stable with depth and snow accumulation. In winter, with less snow, layers, even at the bottom of the snowpack, stay more influenced by meteorological processes. Snow height show strong annual variability, with a decade median peak of 215 cm usually occurring in early March. Maximum observed values range from 147 cm (2025-04-01) to 313 cm (2018-01-23). The timing and extent of peak snow height vary substantially from winter to winter. Snow density ranges from 75.9 to $485.6\,\mathrm{kg\,m^{-3}}$. Fresher deposited snow commonly forms low-density surface layers that are progressively buried and densified throughout the season. This results in a characteristically vertical structure with low densities near the top and denser snow closer to the ground. SSA varies between 6 and $48\,\mathrm{m^2\,kg^{-1}}$. The highest SSA values are seen in freshly deposited surface snow and decrease with depth as snow undergoes grain growth and rounding during metamorphism. Measurements acquired under snow temperatures above approximately $-0.6°C$ should be interpreted with caution because of the temperature-linked retrieval limitations described in Section 3.3. During winter 2023-2024, after 05 April 2024, temperature measurements at depths of 25, 50, and 100 cm begin to reach $0°C$. This date agrees with the SMP-derived SSA increase, with values much higher than those obtained during colder periods, showing the temperature-related behavior found in Section 3.3. Occasional gaps in the density and SSA time series result from a lack of measurements due to instrument issues, incomplete SMP penetration caused by ice layers, or snow depths exceeding the instrument's penetration length.

https://doi.org/10.5194/egusphere-2026-4846
Preprint. Discussion started: 10 September 2026
© Author(s) 2026. CC BY 4.0 License.

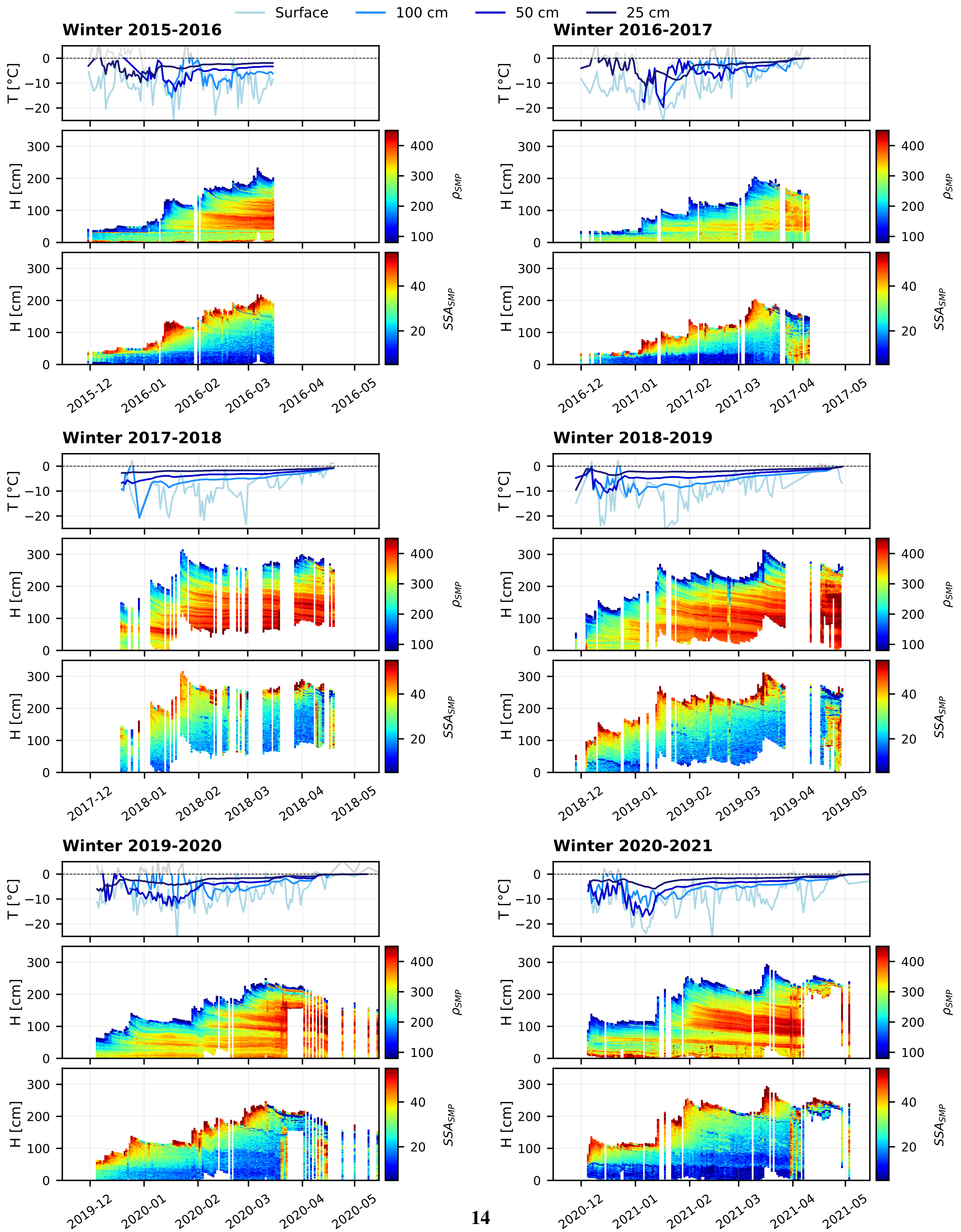

https://doi.org/10.5194/egusphere-2026-4846
Preprint. Discussion started: 10 September 2026
© Author(s) 2026. CC BY 4.0 License.

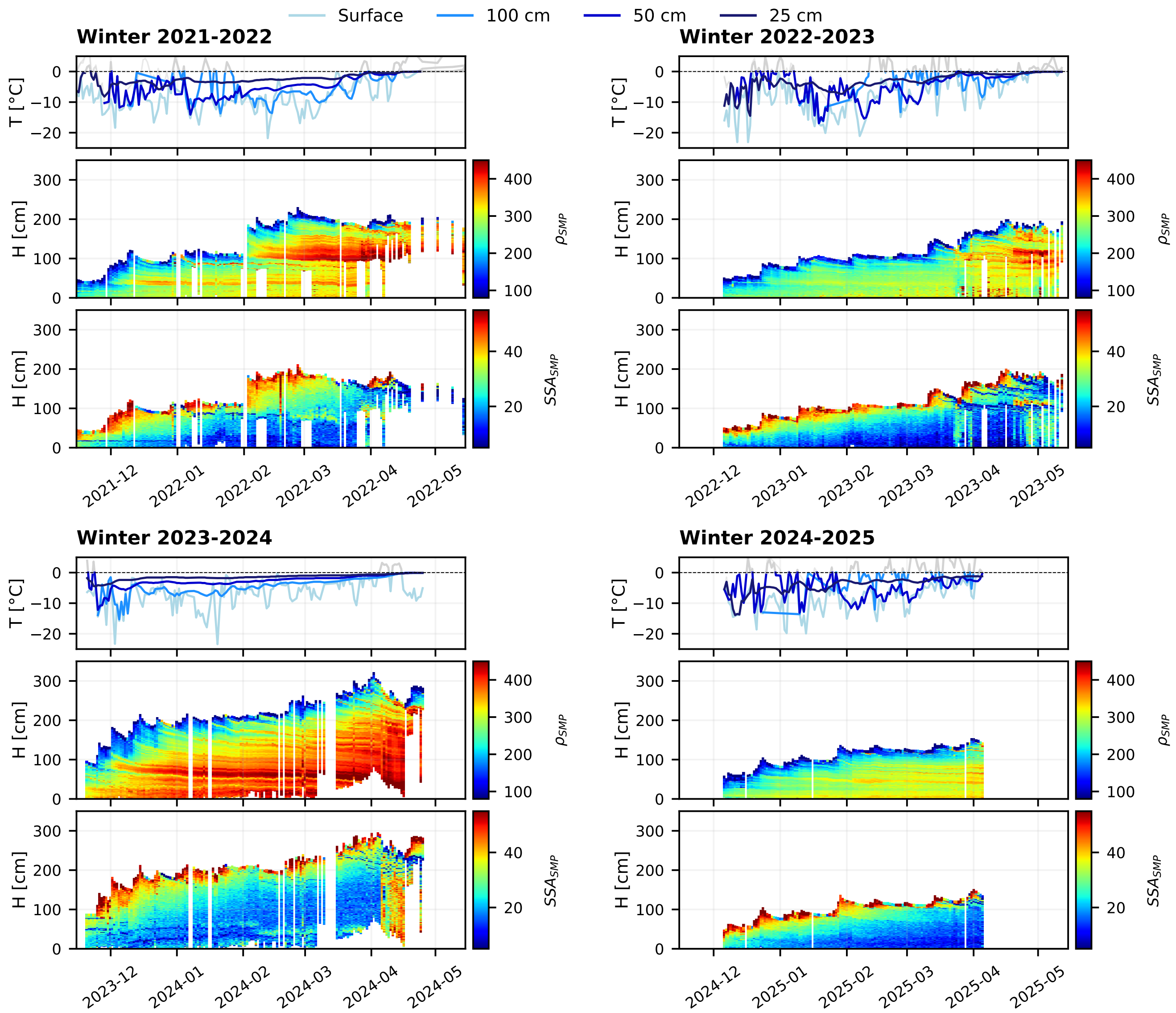

Figure 6. SSA snowpack evolution from 2015–2025. Each panel shows a single winter season, colored by SMP-derived SSA measured along snow height in the lower subplot, and snow temperature at various depths (surface, 25cm, 50cm, 100cm) in the upper subplot.

4 Discussion

285 ### 4.1 A unique long-term dataset for snow microstructure observations

While most studies focus on laboratory experiments or short field campaigns, continuous, daily, high-vertical-resolution observations of snow density and SSA spanning multiple years are rare. The daily SMP observations presented here allow us to investigate snowpack evolution over ten consecutive winters and look at snow stratigraphy at millimeter-scale resolution.

https://doi.org/10.5194/egusphere-2026-4846
Preprint. Discussion started: 10 September 2026
© Author(s) 2026. CC BY 4.0 License.

Combined with long-term meteorological and manual snow observations from the WFJ test site, this is a valuable dataset for studying snowpack evolution across a wide range of environmental conditions.

The ten-year record reveals patterns of snowpack evolution at WFJ that are consistent with known physical snow processes while also capturing inter-annual variability. The rate and type of this metamorphism vary between winters, driven primarily by new snow accumulation, snow depth, thermal and atmospheric processes.

Differences between winters can be understood by looking at snowpack depth and its control on thermal changes. Deeper snowpacks insulate lower layers against surface temperature variations, whereas shallow snowpacks can exhibit stronger temperature gradients. These conditions lead to more isothermal metamorphism and densification, or to temperature-gradient metamorphism and the development of faceted grains and depth hoar. Winter 2015-2016 (Fig. 6) illustrates the extreme of this regime, with persistent low-density layers visible throughout the season that are consistent with the formation of weak layers documented at WFJ during this period by Calonne et al. (2020), which are directly relevant to avalanche formation. Winter 2024-2025 shows less compaction of snow layers closer to the ground, as the shallow snow height results in reduced load and thus densification. This layer variability shows the value of a long continuous record, that individual winters may be unrepresentative of the site's long-term pattern behavior, and that robust characterization of the SSA and density requires sampling throughout the full range of snowpack regimes. Beyond the examples presented here, the processed dataset provides a valuable source for future snow research. The combination of daily temporal and millimeter vertical resolution enables the continuous evolution of individual snow layers to be followed throughout an entire winter. This allows for snow metamorphism to be investigated as a continuous process rather than from isolated observations. Furthermore, the combination of the SMP measurements with long-term meteorological observations, manual snow profiles, and complementary measurements at the WFJ provides an opportunity to directly relate changes in snow microstructure to atmospheric conditions. The dataset therefore has considerable potential for evaluating snowpack models, improving parameterizations of snow density and SSA evolution, investigating inter-annual variability in snowpack properties, and supporting future model developments or validation. As the SMP measurements are still ongoing, its research value for studying long-term changes in seasonal snowpacks will continue to increase.

4.2 Robustness of the CR2020 parameterization

One of the principal findings of this study is that the CR2020 parameterization developed by Calonne et al. (2020) remains remarkably robust when applied to a decade of SMP observations. Although the empirical relationships linking the SMP microstructural parameters to snow density and SSA were calibrated using measurements from winter 2015-2016 during the RHOSSA campaign, the agreement between the retrieved and independently measured snow properties stay close to that reported by Calonne et al. (2020) after accounting for the instrumental force offset and the snow temperature effects. This demonstrates that the parameterization is usable across several snowpacks and meteorological conditions encountered at WFJ. The ten-year dataset also shows that validating empirical parameterizations beyond their original calibration period is important. While the model agrees well for most snow conditions, long-term observations show systematic retrieval biases that are difficult to identify from a single winter alone. In particular, two limitations occur; freshly deposited snow shows larger

https://doi.org/10.5194/egusphere-2026-4846
Preprint. Discussion started: 10 September 2026
© Author(s) 2026. CC BY 4.0 License.

retrieval uncertainties, while snow approaching the melting point experiences a distinct change in mechanical properties that the current retrieval structure does not fully capture. Overall, the present results confirms that the CR2020 parameterization provides reliable estimates of snow density and SSA over a broad range of snow conditions and remains applicable well beyond the dataset on which it was originally developed. At the same time, the long-term observations clearly identify the environmental conditions under which further methodological developments are required.

4.3 Instrumental considerations: offset correction

The increase in force offset observed over the ten winters of SMP measurements (Fig. 2b) indicates a shift in the instrument baseline over time. Thus, long-term SMP datasets cannot be compared across years without correcting the force signal for the RHOSSA calibration offset. The different responses of F_m and L to the offset correction (Fig. 5) arise from the structure of the shot noise model developed by Löwe and van Herwijnen (2012). Whereas an additive offset shifts the mean penetration force F_m almost uniformly throughout the profile, the microstructural length scale depends on both the mean and variance of the force signal.

$$L \propto \left(\frac{\mathrm{Var}(F)}{F_\mathrm{m}^2}\right)^{1/3} \tag{4}$$

An additive offset increases F_m while leaving $\mathrm{Var(F)}$ largely unchanged, since the variance is insensitive to additive constants. As a result, L is much more sensitive to an offset in low-force snow than in high-force snow. Fresh, low-density layers therefore undergo the largest corrections, whereas denser layers are affected only slightly relative to their density. The significance of the correction also depends on the force variance, explaining why some deeper layers can still exhibit noticeable changes. These changes carry into the CR2020 retrieval of snow density and SSA through the logarithmic term F_m and L (Eqs. 2 and 3). Although the logarithmic form captures the nonlinear relationship between the SMP micromechanical parameters and snow properties, it becomes more sensitive for smaller F_m and L. As a result, offset-correction changes are amplified in fresh, low-density snow, where penetration forces are the lowest. The typical density values for fresh snow are found between 50 and $150\,\mathrm{kg\,m^{-3}}$ (Fierz et al., 2009); since uncorrected offsets introduce density biases of up to $50\,\mathrm{kg\,m^{-3}}$, this accounts for a considerable fraction of the common density range for fresh snow. This explains the clear improvement in agreement with HN board density measurements following offset correction (Fig. 3a), with the CCC increasing from 0.26 to 0.53 and the RMSE decreasing from 66.1 to $40.7\,\mathrm{kg\,m^{-3}}$. In contrast, the correction has only a minor influence on comparisons with density cutter and SWE measurements, which mainly sample denser snow where penetration forces are larger, and the relative impact of the offset is correspondingly smaller. For SSA, however, the offset correction generally decreases the retrieved SSA in fresh snow, thereby increasing the apparent underestimation relative to IceCube (Fig. 3b). Nevertheless, the correction is still essential to ensure a consistent instrumental baseline and enable interannual comparison across the ten-year dataset. The remaining SSA bias is discussed in Sect. 4.4.

https://doi.org/10.5194/egusphere-2026-4846
Preprint. Discussion started: 10 September 2026
© Author(s) 2026. CC BY 4.0 License.

4.4 Limitations of the density and SSA parameterization

Two limitations emerge from the ten-year dataset, influencing the retrieval under particularly fresh and warm snow conditions. Despite the offset correction, SMP-derived SSA remains underestimated for values above approximately $40\,\mathrm{m^2\,kg^{-1}}$ (Fig. 3b) in both the calibration and validation winters. Because this bias is already present in the 2015-2016 calibration dataset and is unaffected by the offset correction, it cannot be attributed to instrumental offset or drift. In addition, IceCube measurements may carry an increasing uncertainty for SSA values above approximately $60\,\mathrm{m^2\,kg^{-1}}$, where the low optical depth of fresh, low-density snow can lead to an overestimation of SSA (Gallet et al., 2009). Another possible explanation is that freshly deposited snow produces penetration forces close to the instrumental noise (±5 mN), limiting the information available to estimate F_m and L precisely. Addressing this limitation would require recalibrating the parametrization or developing a new model to obtain the micromechanical parameters using low-uncertainty reference measurements, such as micro-computed tomography (Heggli et al., 2011; Proksch et al., 2016), specifically for fresh snow conditions.

A second limitation appears as the snow temperature approaches the melting point. An empirical transition occurs at -0.6 ± 0.2°C, above which the gradual temperature dependence of the SMP micro-mechanical parameters changes rapidly. Under this threshold, F_m and L evolve gradually, with L increasing between approximately -6°C and -0.6°C, consistent with the expected coarsening of the snow microstructure during snow metamorphism. Above the threshold, L decreases abruptly while F_m increases, resulting in a strong increase in the SSA retrieved by CR2020 and a deterioration in agreement with the independent reference measurements. In cold snow, the SMP force record consists of several discrete rupture events as the probe tip fractures inter-grain bonds as defined by Löwe and van Herwijnen (2012). These force fluctuations provide the statistical information used in the shot noise model to estimate L. As snow approaches 0°C, its mechanical response changes. Inter-grain bonds soften and partially melt, shifting the mechanical response from brittle fracture toward more viscous deformation (Scapozza and Bartelt, 2003). Therefore F_m increases as the probe encounters more resistance from the denser snow, usually located at the bottom of the snowpack, while, $\mathrm{Var(F)}$ decreases, as bond fractures become less distinct. Within the shot noise model, both changes reduce L (Eq. 4). While a gradual change in mechanical response of warm snow is expected, the abrupt decrease in L observed near -0.6°C is inconsistent with gradual microstructure evolution due to metamorphism. Instead, it suggests that the force signal no longer satisfies the assumptions underlying the shot noise model. These changes of the parameters L and F_m at temperatures close to the melting point propagate differently into the obtained density and SSA. Because density depends on F_m and L through a mixed term that partially self-compensates (Eq. 3), minor density deviations are observed as temperature increases and remain within plausible ranges even near the threshold. SSA, through its strong logarithmic dependence on L alone, amplifies the rapid drop in L into a strong increase in SSA, which is not consistent with the expected gradual evolution of snow microstructure. This makes SSA a more sensitive derived quantity than density to temperature shifts trough the shot noise model. We also briefly investigated the influence of grain type by matching SMP profiles with the manually recorded grain classifications available bi-monthly at the WFJ site. Similar behavior, including the sharp decrease in L at -0.6 °C, was observed when the analysis was restricted to rounded grains and melt forms. This suggests that the observed threshold is not an artifact of changing grain type, but is associated with the temperature dependence of

https://doi.org/10.5194/egusphere-2026-4846
Preprint. Discussion started: 10 September 2026
© Author(s) 2026. CC BY 4.0 License.

the SMP retrieval. For the WFJ dataset, this mainly affects measurements in April and May, coinciding with the shift of the snowpack toward wet snow metamorphism. To extend the SMP retrieval reliably for melt-season measurements, a new parameterization would be required, potentially based on laboratory experiments comparing the force-signal statistics of cold versus near-melting snow. However, this approach is highly questionable, as the force signal may strongly depend on liquid water content (LWC), in addition to density and SSA, introducing an additional dependency that increases complexity.

Fig. 7 shows the joint density distribution of SMP-derived SSA and density over 10 winters, with the colored background showing the manually bi-monthly measured temperature and the monthly median evolution plotted on top. This figure shows the seasonal and inter-annual effects of this limitation. The median monthly trajectory reveals the expected inverse relationship between SSA and density associated with snow metamorphism (Braun et al., 2026). From early winter until March, the monthly median follows a seasonal trajectory towards decreasing SSA and increasing density, indicating the progressive transformation of fresh snow through compaction and grain growth. In April and May, the trajectory departs from this seasonal evolution, with SSA increasing sharply while the density stays rougly constant or continues to increase. This departure coincides with the near melting point regime in which the abrupt changes in F_m and L and the resulting instability of the shot noise retrieval are observed. The figure therefore demonstrates the consequence of this limitation at the decadal scale. The apparent increase in spring SSA is not consistent with the expected seasonal evolution of snow microstructure, but results from the temperature-dependent instability of the SMP retrieval. When measurements above -0.6°C are excluded, the monthly trajectory stays within the physically consistent range observed during the colder part of the season, further supporting this interpretation.

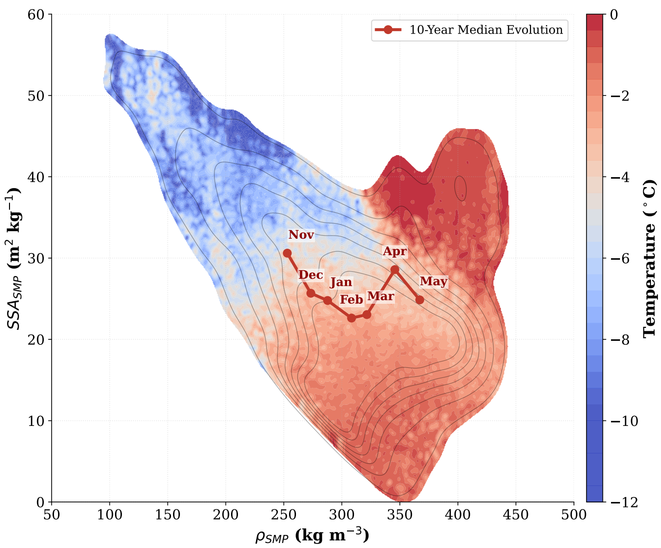

Figure 7. Joint kernel density distribution of SMP-derived SSA and snow density across the ten winters (2015–2025). The background represents the manually measured bi-monthly mean snow temperature, and the red line shows the monthly median trajectory.

https://doi.org/10.5194/egusphere-2026-4846
Preprint. Discussion started: 10 September 2026
© Author(s) 2026. CC BY 4.0 License.

5 Conclusions

We presented a unique ten-year dataset of daily SMP measurements at the Weissfluhjoch research site with high temporal and vertical resolution, spanning the winters 2015-2016 to 2024-2025. Comparison of SMP-derived density and SSA against independent reference measurements (density cutters, SWE-derived profiles, new snow measurements, IceCube) show that the CR2020 parameterization, originally derived during the winter 2015-2016 RHOSSA campaign, remains usable across the ten-year dataset and provides reliable estimates for density and SSA ranges typical of seasonal snowpacks. For long-term SMP observations, the instrumental force offset should be accounted and corrected to the RHOSSA reference value, particularly because its effect is strongest in fresh, low-density snow. The force offset increased systematically over the ten years, resulting in density overestimation and affecting the retrieved SSA, with the largest effects in low-force near-surface layers. Applying the offset correction reduced the density overestimation in fresh snow and increased agreement with HN board measurements, while also providing a consistent instrumental baseline for inter-annual comparison across the ten winters. In contrast, the persistent underestimation of SSA above approximately $40\,\mathrm{m^2\,kg^{-1}}$ remained after correction and is therefore not attributable to the instrumental offset. This indicates that the high-SSA scatter shows a separate limitation of the retrieval under very fresh, low-force conditions and could also be attributed to uncertainties in the reference measurements themselves. In this study, drift had a negligible effect on the retrieved snow properties, but its influence should nevertheless be evaluated when applying the approach to other long-term SMP datasets. A second limitation occurs under near-melting conditions. At approximately -0.6 ± 0.2°C, an abrupt decrease in L and increase in F_m lead to unrealistically high SSA estimates. This behavior likely reflects a change in the mechanical response of warm snow, potentially associated with a transition from brittle fracture to more viscous deformation and the presence of liquid water, making the assumptions underlying the shot noise model less valid. Density is less affected by this transition due to partial compensation between F_m and L in the CR2020 parameterization. Measurements above this temperature should therefore be interpreted with caution under the current retrieval framework. After accounting for the instrumental offset and the warm-snow limitation, the ten-year record shows consistent seasonal evolution of snow properties, characterized by decreasing SSA and increasing density from early winter through spring, together with inter-annual variability. The dataset therefore provides not only a long-term characterization of snow microstructure at Weissfluhjoch, but also a valuable reference for evaluating snowpack models and developing improved descriptions of snow density and SSA evolution. Extending reliable SMP retrievals to very fresh and near-melting snow will require targeted reference measurements and controlled experiments to better characterize the SMP force response under these conditions.

Data availability. The dataset used in the paper is available on the EnviDat database https://www.doi.org/10.16904/envidat.641 (Löwe et al., 2025)

Author contributions. LGF performed the analysis and wrote the first version of the paper. BW and BR contributed to the interpretation of the results and to the writing. All authors reviewed and revised the manuscript. BW directed the project.

© Author(s) 2026. CC BY 4.0 License.

Competing interests. The authors declare that they have no conflict of interest.

440 *Acknowledgments.* The authors would like to thank the PhD students from SLF, without whom collecting this dataset would not have been possible. We thank Dr. Matthias Jaggi for his instrumental expertise. We thank Martin Proksch and Benjamin Reuter (SLF), who initiated the campaign of daily SMP measurements. The AI tools ChatGPT (OpenAI) and Grammarly were used to assist with language editing, including grammar correction and reformulation.

https://doi.org/10.5194/egusphere-2026-4846
Preprint. Discussion started: 10 September 2026
© Author(s) 2026. CC BY 4.0 License.

References

Bormann, K. J., Westra, S., Evans, J. P., and McCabe, M. F.: Spatial and temporal variability in seasonal snow density, Journal of Hydrology, 484, 63–73, https://doi.org/10.1016/j.jhydrol.2013.01.032, 2013.

Braun, A., Fourteau, K., Frei, S., Lehning, M., and Löwe, H.: Toward a physically and microstructure-based equation for the evolution of the specific surface area in snow, Journal of Glaciology, 72, e40, https://doi.org/10.1017/jog.2024.109, 2026.

Calonne, N., Flin, F., Geindreau, C., Lesaffre, B., and Rolland Du Roscoat, S.: Study of a temperature gradient metamorphism of snow from 3-D images: time evolution of microstructures, physical properties and their associated anisotropy, The Cryosphere, 8, 2255–2274, https://doi.org/10.5194/tc-8-2255-2014, 2014.

Calonne, N., Richter, B., Löwe, H., Cetti, C., Ter Schure, J., Van Herwijnen, A., Fierz, C., Jaggi, M., and Schneebeli, M.: The RHOSSA campaign: multi-resolution monitoring of the seasonal evolution of the structure and mechanical stability of an alpine snowpack, The Cryosphere, 14, 1829–1848, https://doi.org/10.5194/tc-14-1829-2020, 2020.

Carroll, T.: A Comparison of the CRREL 500 cm^3 Tube and the ILTS 200 and 100 cm^3 Box Cutters Used for Determining Snow Densities, Journal of Glaciology, 18, 334–337, https://doi.org/10.3189/S0022143000021420, 1977.

Conger, S. M. and McClung, D. M.: Comparison of density cutters for snow profile observations, Journal of Glaciology, 55, 163–169, https://doi.org/10.3189/002214309788609038, 2009.

Dominé, F., Cabanes, A., Taillandier, A.-S., and Legagneux, L.: Specific Surface Area of Snow Samples Determined by CH_4 Adsorption at 77 K and Estimated by Optical Microscopy and Scanning Electron Microscopy, Environmental Science & Technology, 35, 771–780, https://doi.org/10.1021/es001168n, 2001.

Dozier, J., Bair, E. H., and Davis, R. E.: Estimating the spatial distribution of snow water equivalent in the world's mountains, WIREs Water, 3, 461–474, https://doi.org/10.1002/wat2.1140, 2016.

Fierz, C.: WFJ2: Snow measurements from the Weissfluhjoch research site, Davos, https://doi.org/10.16904/ENVIDAT.516, artwork Size: 54473566 bytes Pages: 54473566 bytes, 2019.

Fierz, C., Armstrong, R. L., Durand, Y., Etchevers, P., Greene, E., M. McClung, D., Nishimura, K., K. Satyawali, P., and A. Sokratov, S.: Classification for Seasonal Snow on the Ground, vol. IACS contribution of *IHP-VII Technical Documents in Hydrology*, UNESCO-IHP, Paris, 2009.

for Snow and Avalanche Research SLF, W. I.: SnowMicroPen® 5 (SMP5), https://www.wsl.ch/de/services-produkte/snowmicropen-smp5-version/, 2023.

Gallet, J.-C., Domine, F., Zender, C. S., and Picard, G.: Measurement of the specific surface area of snow using infrared reflectance in an integrating sphere at 1310 and 1550 nm, The Cryosphere, 3, 167–182, https://doi.org/10.5194/tc-3-167-2009, 2009.

Gergely, M., Wolfsperger, F., and Schneebeli, M.: Simulation and Validation of the InfraSnow: An Instrument to Measure Snow Optically Equivalent Grain Size, IEEE Transactions on Geoscience and Remote Sensing, 52, 4236–4247, https://doi.org/10.1109/TGRS.2013.2280502, 2014.

Hagenmuller, P., Matzl, M., Chambon, G., and Schneebeli, M.: Sensitivity of snow density and specific surface area measured by microtomography to different image processing algorithms, The Cryosphere, 10, 1039–1054, https://doi.org/10.5194/tc-10-1039-2016, 2016.

Heggli, M., Köchle, B., Matzl, M., Pinzer, B., Riche, F., Steiner, S., Steinfeld, D., and Schneebeli, M.: Measuring snow in 3-D using X-ray tomography: assessment of visualization techniques, Annals of Glaciology, 52, 231–236, https://doi.org/10.3189/172756411797252202, 2011.

Intercantonal Measurement and Information System IMIS: IMIS measuring network, https://doi.org/10.16904/ENVIDAT.406, artwork Size: 11294 bytes, 1 bytes, 1 bytes Pages: 11294 bytes, 1 bytes, 1 bytes, 2023.

Johnson, J. B. and Schneebeli, M.: Characterizing the microstructural and micromechanical properties of snow, Cold Regions Science and Technology, 30, 91–100, https://doi.org/10.1016/S0165-232X(99)00013-0, 1999.

Kaasik, M., Meinander, O., Leppänen, L., Anttila, K., Dagsson-Waldhauserova, P., Ginnerup, A., Hampinen, T., Liu, Y., Gunnarsson, A., Langley, K., and Arslan, A. N.: Accuracy of Manual Snow Sampling, Depending on the Sampler's Cross-Section—A Comparative Study, Geosciences, 13, 205, https://doi.org/10.3390/geosciences13070205, 2023.

Legagneux, L., Cabanes, A., and Dominé, F.: Measurement of the specific surface area of 176 snow samples using methane adsorption at 77 K, Journal of Geophysical Research: Atmospheres, 107, https://doi.org/10.1029/2001JD001016, 2002.

Legagneux, L., Taillandier, A.-S., and Domine, F.: Grain growth theories and the isothermal evolution of the specific surface area of snow, Journal of Applied Physics, 95, 6175–6184, https://doi.org/10.1063/1.1710718, 2004.

Liston, G. E., Haehnel, R. B., Sturm, M., Hiemstra, C. A., Berezovskaya, S., and Tabler, R. D.: Simulating complex snow distributions in windy environments using SnowTran-3D, Journal of Glaciology, 53, 241–256, https://doi.org/10.3189/172756507782202865, 2007.

Löwe, H. and van Herwijnen, A.: A Poisson shot noise model for micro-penetration of snow, Cold Regions Science and Technology, 70, 62–70, https://doi.org/10.1016/j.coldregions.2011.09.001, 2012.

Löwe, H., Proksch, M., Reuter, B., Calonne, N., Richter, B., Jaggi, M., Mewes, L., Schneebeli, M., Dadic, R., and Walter, B.: WFJ_DailySMP - High-Resolution Snow Stratigraphy at Weissfluhjoch – Davos 2015-ongoing, https://doi.org/10.16904/ENVIDAT.641, artwork Size: 5388036473 bytes Pages: 5388036473 bytes, 2025.

Magnusson, J. and Jonas, T.: Dataset on new snow water equivalent, https://doi.org/10.16904/ENVIDAT.590, artwork Size: 126716 bytes Pages: 126716 bytes, 2025.

Marty, C.: GCOS SWE data from 11 stations in Switzerland, https://doi.org/10.16904/15, artwork Size: 8049 bytes, 343040 bytes Pages: 8049 bytes, 343040 bytes, 2020.

Marty, C., Rohrer, M. B., Huss, M., and Stähli, M.: Multi-decadal observations in the Alps reveal less and wetter snow, with increasing variability, Frontiers in Earth Science, 11, 1165 861, https://doi.org/10.3389/feart.2023.1165861, 2023.

Matzl, M. and Schneebeli, M.: Measuring specific surface area of snow by near-infrared photography, Journal of Glaciology, 52, 558–564, https://doi.org/10.3189/172756506781828412, 2006.

Mewes, L., Löwe, H., Schneebeli, M., and Walter, B.: Optical determination of snow density via sub-surface scattering, Communications Physics, 9, 57, https://doi.org/10.1038/s42005-026-02490-1, 2026.

Miot, M., Wautier, A., Polfer, P., Philippe, P., Fülöp, T., and Nicot, F.: Mechanics of densely packed snow across scales: A constitutive modelling strategy based on the 3-D H-model, Journal of Glaciology, 71, e62, https://doi.org/10.1017/jog.2024.112, 2025.

Poschlod, B. and Daloz, A. S.: Snow depth in high-resolution regional climate model simulations over southern Germany – suitable for extremes and impact-related research?, The Cryosphere, 18, 1959–1981, https://doi.org/10.5194/tc-18-1959-2024, 2024.

Proksch, M., Löwe, H., and Schneebeli, M.: Density, specific surface area, and correlation length of snow measured by high-resolution penetrometry, Journal of Geophysical Research: Earth Surface, 120, 346–362, https://doi.org/10.1002/2014JF003266, 2015.

https://doi.org/10.5194/egusphere-2026-4846
Preprint. Discussion started: 10 September 2026
© Author(s) 2026. CC BY 4.0 License.

Proksch, M., Rutter, N., Fierz, C., and Schneebeli, M.: Intercomparison of snow density measurements: bias, precision, and vertical resolution, The Cryosphere, 10, 371–384, https://doi.org/10.5194/tc-10-371-2016, 2016.

Scapozza, C. and Bartelt, P. A.: The influence of temperature on the small-strain viscous deformation mechanics of snow: a comparison with polycrystalline ice, Annals of Glaciology, 37, 90–96, https://doi.org/10.3189/172756403781815410, 2003.

Schweizer, J., Bruce Jamieson, J., and Schneebeli, M.: Snow avalanche formation, Reviews of Geophysics, 41, 2002RG000 123, https://doi.org/10.1029/2002RG000123, 2003.

Van Herwijnen, A. and Jamieson, B.: Fracture character in compression tests, Cold Regions Science and Technology, 47, 60–68, https://doi.org/10.1016/j.coldregions.2006.08.016, 2007.

Walter, B., Weigel, H., Wahl, S., and Löwe, H.: Wind tunnel experiments to quantify the effect of aeolian snow transport on the surface snow microstructure, The Cryosphere, 18, 3633–3652, https://doi.org/10.5194/tc-18-3633-2024, 2024.

Zuanon, N.: IceCube, a portable and reliable instrument for snow specific surface area measurement in the field, https://www.semanticscholar.org/paper/IceCube%2C-a-portable-and-reliable-instrument-for-in-Zuanon/2575ab70132960e6e27b72c8e1b1d05a68450628, 2013.